Cell Reports

Article

# A transepithelial pathway delivers succinate to macrophages, thus perpetuating their pro-inflammatory metabolic state

## Graphical abstract

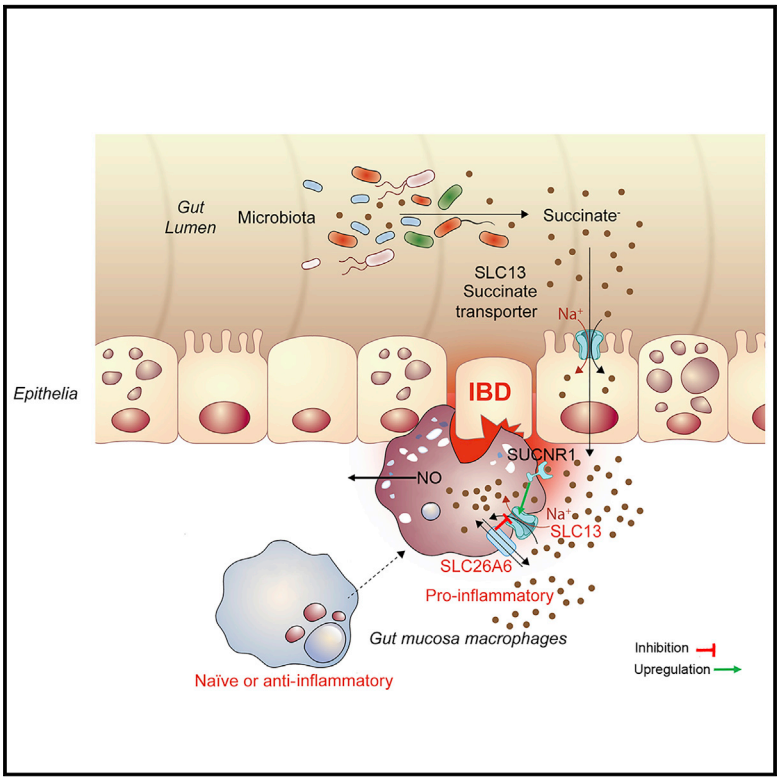


## Highlights

- Succinate uptake is elevated in macrophages to perpetuate their pro-inflammatory state
- $Na^+$-dependent transporters mediate transepithelial succinate delivery into macrophages
- Succinate concentrations are elevated in the serum and feces of IBD patients
- Succinate-metabolizing bacteria are altered in IBD patients


## Authors

Moran Fremder, Seung Won Kim, Ahlam Khamaysi, ..., Uzi Hadad, Jae Hee Cheon, Ehud Ohana

## Correspondence

geniushee@yuhs.ac (J.H.C.), ohanaeh@bgu.ac.il (E.O.)



## In brief

Succinate is emerging as a prominent pro-inflammatory metabolite. Fremder et al. show that transporter-mediated succinate uptake into macrophages is elevated to enhance and perpetuate inflammation. In IBD, high succinate metabolized by distinct gut bacteria may cause chronic inflammation. Hence, this pathway is a potential therapeutic target to treat inflammatory diseases.


Fremder et al., 2021, Cell Reports *36*, 109521
August 10, 2021 
https://doi.org/10.1016/j.celrep.2021.109521

CellPress

Cell Reports

CellPress
OPEN ACCESS

Article

# A transepithelial pathway delivers succinate to macrophages, thus perpetuating their pro-inflammatory metabolic state

Moran Fremder,[1,6] Seung Won Kim,[2,3,4,6] Ahlam Khamaysi,[1] Liana Shimshilashvili,[1] Hadar Eini-Rider,[1] I Seul Park,[2,3] Uzi Hadad,[5] Jae Hee Cheon,[2,3,4,7,*] and Ehud Ohana[1,7,8,*]

[1]Department of Clinical Biochemistry and Pharmacology, Faculty of Health Sciences, Ben-Gurion University of the Negev, Beer-Sheva, Israel
[2]Department of Internal Medicine and Institute of Gastroenterology, Yonsei University College of Medicine, Seoul, Korea
[3]Brain Korea 21 PLUS Project for Medical Science, Yonsei University College of Medicine, Seoul, Korea
[4]Severance Biomedical Science Institute, Yonsei University College of Medicine, Seoul, Korea
[5]The Ilse Katz Institute for Nanoscale Science and Technology Ben-Gurion University of the Negev, Beer-Sheva, Israel
[6]These authors contributed equally
[7]These authors contributed equally
[8]Lead contact
*Correspondence: geniushee@yuhs.ac (J.H.C.), ohanaeh@bgu.ac.il (E.O.)
https://doi.org/10.1016/j.celrep.2021.109521

## SUMMARY

The gut metabolite composition determined by the microbiota has paramount impact on gastrointestinal physiology. However, the role that bacterial metabolites play in communicating with host cells during inflammatory diseases is poorly understood. Here, we aim to identify the microbiota-determined output of the pro-inflammatory metabolite, succinate, and to elucidate the pathways that control transepithelial succinate absorption and subsequent succinate delivery to macrophages. We show a significant increase of succinate uptake into pro-inflammatory macrophages, which is controlled by $Na^+$-dependent succinate transporters in macrophages and epithelial cells. Furthermore, we find that fecal and serum succinate concentrations were markedly augmented in inflammatory bowel diseases (IBDs) and corresponded to changes in succinate-metabolizing gut bacteria. Together, our results describe a succinate production and transport pathway that controls the absorption of succinate generated by distinct gut bacteria and its delivery into macrophages. In IBD, this mechanism fails to protect against the succinate surge, which may result in chronic inflammation.

## INTRODUCTION

The epithelium of the gastrointestinal (GI) tract absorbs nutrients and minerals but also acts as the main barrier that protects against the penetration of pathogens. Damage to the epithelium may lead to severe infections by pathogens, inflammation, loss of minerals, and hampered metabolite absorption and secretion. This occurs in several pathologies, most notably, inflammatory bowel diseases (IBDs), namely, Crohn's disease (CD) and ulcerative colitis (UC). Although the etiology of IBD has not been fully established, it is known that it is associated with impaired epithelial barrier function and activated immune cells in the gut mucosa that produce excessive amounts of pro-inflammatory mediators (Onizawa et al., 2009; Plevy et al., 1997; Schmitz et al., 1999). Current treatments for active IBD include anti-inflammatory drugs, immunomodulators, and/or biological agents (Colombel et al., 2010; Nielsen and Ainsworth, 2013).

Implicated in the pathogenesis of several diseases, including IBD, obesity, and some allergic disorders, is an imbalance in the intestinal microbiota, termed "dysbiosis" (DeGruttola et al., 2016). Therefore, characterization of the gut microbiome and its alteration in diseases have emerged as areas of intensive research. It has thus been shown that microbial-secreted metabolites regulate colonic homeostasis by stimulating specific receptors (Smith et al., 2013). Metabolite-sensing receptors and metabolite transport proteins are highly expressed both on the gut epithelia and also on macrophages (Niess and Adler, 2010; Niess et al., 2005). Nevertheless, the role that metabolites produced by the gut microbiome play in the pathogenesis of IBD is less investigated.

On one hand, the metabolic intermediate, succinate, has been shown to play a key role in intestinal homeostasis and energy metabolism, but on the other hand, succinate also acts as a pro-inflammatory metabolite. Notably, cytoplasmic succinate accumulation stabilizes hypoxia-inducible factor 1α (HIF-1α), shifting macrophages to glycolysis and to a pro-inflammatory state (Tannahill et al., 2013). In mammalian cells, the cytoplasmic succinate levels are determined by mitochondrial succinate production in the TCA cycle, driven by glutamine-dependent anaplerosis. However, extracellular succinate uptake

mediated by members of the $Na^+$-dependent SLC13 family of transporters is another pivotal source for intracellular succinate. It has been previously shown that succinate uptake into mouse intestinal tissue is indeed $Na^+$ dependent and involves the orchestrated function of SLC13 transporters (Browne et al., 1978; Ohana et al., 2013; Pajor, 1995). In addition, the major succinate transporter, SLC13A2, is strongly inhibited by the SLC26A6 transporter through interaction. Thus, the SLC13/SLC26 complex strictly regulates succinate homeostasis (Khamaysi et al., 2019; Ohana et al., 2013). Hence to reabsorb succinate across epithelial cell membranes, SLC13 transporters mediate succinate influx, and the organic anion transporters (OATs) mediate succinate efflux via an organic anion/carboxylic acid exchange mechanism (Emami Riedmaier et al., 2012). For example, the major basolateral transporters that mediate succinate extrusion in the proximal tubule epithelia are the OAT 1 and 3 (Kojima et al., 2002; Lungkaphin et al., 2006). The OAT 10 transporter mediates succinate extrusion via the apical membrane and was shown to express in the kidney and colon (Wang and Sweet, 2013). In the colorectal Caco-2 cells, succinate influx was shown to be mediated mainly by SLC13A2, which is highly selective to succinate, and also by SLC13A5, which is more selective to citrate than to succinate (Weerachayaphorn and Pajor, 2008). An OAT transporter, likely OAT4, that mediates the transport of methylsuccinate, but not succinate, was also found in Caco-2 cells.

Succinate acts as a pivotal metabolic signaling molecule via stimulation of the succinate-specific G protein-coupled receptor, succinate receptor (SUCR1, GPR91, or SUCNR1). The SUCNR1 has been shown to be expressed in several tissues and cells, including hepatic stellate cells (De Minicis et al., 2007), human monocyte-derived dendritic cells (MoDCs), and in the epithelia of the intestine and kidney, where SUCNR1 stimulation regulates SLC13, but not OAT, function (Khamaysi et al., 2019; Toma et al., 2008). The expression of SUCNR1 is increased in pro-inflammatory macrophages (Littlewood-Evans et al., 2016), and several studies have reported that SUCNR1 stimulation by elevated extracellular succinate amplifies the pro-inflammatory state in macrophages (Littlewood-Evans et al., 2016) and in dendritic cells (Rubic et al., 2008). Another study showed that immature MoDCs (iMoDCs) migrate in response to succinate in a dose-dependent manner, with $Sucnr1^{-/-}$ mice exhibiting impaired migration of dendritic cells and a diminished immune response (Rubic et al., 2008). In neural stem cells, SUCNR1 stimulation activates scavenging of the pro-inflammatory succinate, thus resulting in lower succinate to reduce inflammation (Peruzzotti-Jametti et al., 2018). Intestinal tuft cells utilize SUCNR1 to detect succinate secreted by bacterial and parasitic infection to activate a secondary immune response (Lei et al., 2018). In contrast, a more recent study suggests that SUCNR1 stimulation in adipose tissue-resident macrophages may trigger an anti-inflammatory response (Keiran et al., 2019). Together, these studies indicate that elevated intracellular succinate is an obligatory pro-inflammatory signal. However, although extracellular succinate generally amplifies pro-inflammatory responses, under specific conditions it may also act as an anti-inflammatory signal. Remarkably, in IBD, SUCNR1 promotes inflammation, because Sucnr1 deletion in mice protects against symptoms of induced colitis and intestinal fibrosis (Macias-Ceja et al., 2019).

A particular aspect of succinate homeostasis is the role of altered microbiota-produced succinate transport in sustaining inflammation, which is the main focus of our study. Elevated cytoplasmic succinate concentrations facilitate pro-inflammatory macrophage polarization and plasticity. Hence transporter-mediated absorption of luminal succinate may play a key role in either triggering or maintaining the GI symptoms of IBD and related disorders. Therefore, we asked: what is the role of transepithelial absorption of microbiota-generated succinate in controlling succinate delivery into macrophages in IBD?

## RESULTS

### Succinate uptake into macrophages is augmented by lipopolysaccharides/interferon γ (LPS/IFNγ) treatment

A succinate-rich environment can potentially contribute to chronic inflammation, because both intracellular and extracellular succinate induce and maintain the pro-inflammatory state of macrophages (Tannahill et al., 2013). To determine whether succinate uptake into macrophages is affected by macrophage polarization, we monitored succinate uptake into three different macrophage populations of either primary bone marrow-derived macrophages (BMDMs) or RAW264.7 cell line, as indicated in Figure 1. Our results show that succinate uptake into LPS/IFNγ-treated pro-inflammatory macrophages is significantly elevated in a time-dependent manner. In fact, the uptake increased as high as 5.5-fold in LPS/IFNγ-treated BMDMs that were cultured in macrophage colony-stimulating factor (M-CSF) media, compared with naive and interleukin (IL)-4/IL-13-treated cells (Figure 1A, 45 min of uptake). The uptake into BMDMs that were cultured in granulocyte-macrophage colony-stimulating factor (GM-CSF) showed a 1.5-fold increase after 45 min of incubation with succinate (Figure 1B). The inflammatory state of the M-CSF-treated macrophage culture was confirmed by nitric oxide (NO) secretion assay that showed a dramatic elevation of NO secretion in LPS/IFNγ-treated macrophages compared with the naive and IL-4/IL-13-treated populations (Figure 1C). In addition, we monitored $CD11b^+$ and F4/80 (Figure S1A) or CD80 (Figure S1B) expression by flow cytometry, as well as CD206 (Figure S1C) and IL-1β (Figure S1D) expression by western blot analysis, that further verified the inflammatory state of the macrophage cultures that were described in Figure 1. In RAW264.7 cells, we measured an almost 3-fold increase in succinate uptake compared with the naive or the anti-inflammatory IL-4/IL-13-treated populations (Figure 1D) under conditions similar to those described in Figure 1B. Because elevated cytoplasmic succinate re-programs macrophages to the pro-inflammatory state (Tannahill et al., 2013), we measured the effect of extracellular succinate on the inflammatory state by monitoring NO secretion in the presence or absence of succinate. To attenuate intracellular succinate production, we stimulated the macrophages for 16 h in media containing LPS/IFNγ and extracellular succinate. Then, the culture was washed and incubated for 50 h in the absence of L-glutamine with or without succinate, as indicated. We found that in the presence of extracellular succinate in the media, NO secretion was progressively elevated up

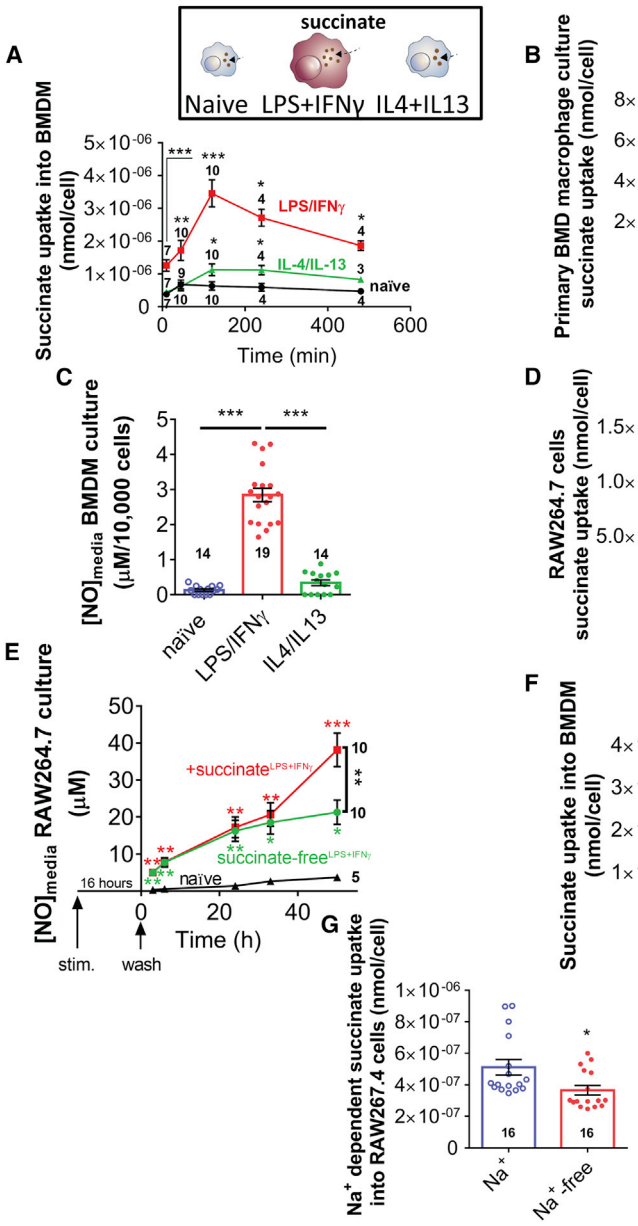


**Figure 1. The $Na^+$-dependent uptake of succinate into LPS/IFNγ-treated cells is higher than the uptake into other macrophage populations**

(A and B) Succinate uptake measured in treated BMDMs.

Notably, LPS/IFNγ-treated macrophages show higher succinate uptake compared with naive and IL-4/IL-13-treated macrophages.

(C) The results in (A and B) correlate with elevated NO secretion (C) in the pro-inflammatory population.

(D) Similarly, succinate uptake was increased in LPS/IFNγ-treated RAW264.7 cell culture.

(E) RAW264.7 cells were stimulated in a glutamine-containing media in the presence of 5 mM $Na^+$-succinate. Subsequently, the cultures were washed and incubated in glutamine-free media in the presence (+succinate) or absence (succinate-free) of succinate, and NO concentrations were monitored at different time points.

(F and G) Succinate uptake was monitored in the presence or absence of $Na^+$ in either BMDMs (F) or RAW264.7 cells (G), as indicated in the figure.

Data are shown as means ± SEM. Statistical significance was assessed either with t test or one-way ANOVA followed by Tukey's or Holm-Sidak's post-test. *p < 0.05, **p < 0.01, ***p < 0.001.

to an approximately 2.5-fold increase compared with the NO levels monitored in succinate-free media (Figure 1E). This suggests that extracellular succinate uptake exacerbates the inflammatory function of macrophages over time. To determine whether succinate uptake into macrophages is mediated by the $Na^+$-dependent SLC13 transporters, we monitored BMDM succinate uptake in the presence or absence of $Na^+$ (Figure 1F). We found that background succinate uptake in naive cells was $Na^+$ independent, while the increased uptake in LPS/IFNγ-treated cells was dramatically reduced in the absence of $Na^+$ (Figure 1F). This suggests that a significant portion of succinate uptake by pro-inflammatory macrophages is $Na^+$ dependent. Finally, we found a 30% decrease in the uptake of succinate into LPS/IFNγ-treated RAW264.7 cells that were incubated in a $Na^+$-free solution compared with that monitored in $Na^+$-containing solution (Figure 1G). These findings suggest that the uptake of succinate into pro-inflammatory macrophages is significantly elevated compared with either naive or anti-inflammatory polarized macrophages. The elevated succinate uptake into macrophages is mediated by a $Na^+$-dependent transport mechanism, most likely by a single or several members of the SLC13 family that act as $Na^+$-dependent succinate/citrate transporters, namely, SLC13A2, SLC13A3, or SLC13A5.

Therefore, we aimed to identify how the SLC13 transporter-mediated succinate uptake into macrophages is regulated. We have previously shown that stimulation of SUCNR1 by succinate regulates both SLC13A2 and SLC13A3, which are more selective to succinate but also mediate citrate transport (Khamaysi et al., 2019). Therefore, to discern SUCNR1 stimulation from SLC13 transport function, we monitored citrate uptake into LPS/IFNγ-treated RAW264.7 cells in the presence or absence of either 250 μM succinate or the SLC13A5-specific inhibitor, BI01383298 (10 μM) (Higuchi et al., 2020). Our results in Figure 2A indicate that the addition of 250 μM succinate elevated citrate uptake into stimulated macrophages, likely by stimulating SUCNR1, the expression of which is augmented in LPS/IFNγ-stimulated macrophages (Figure 2B; Littlewood-Evans et al., 2016). Nonetheless, the SLC13A5 inhibitor had no effect on citrate uptake, suggesting

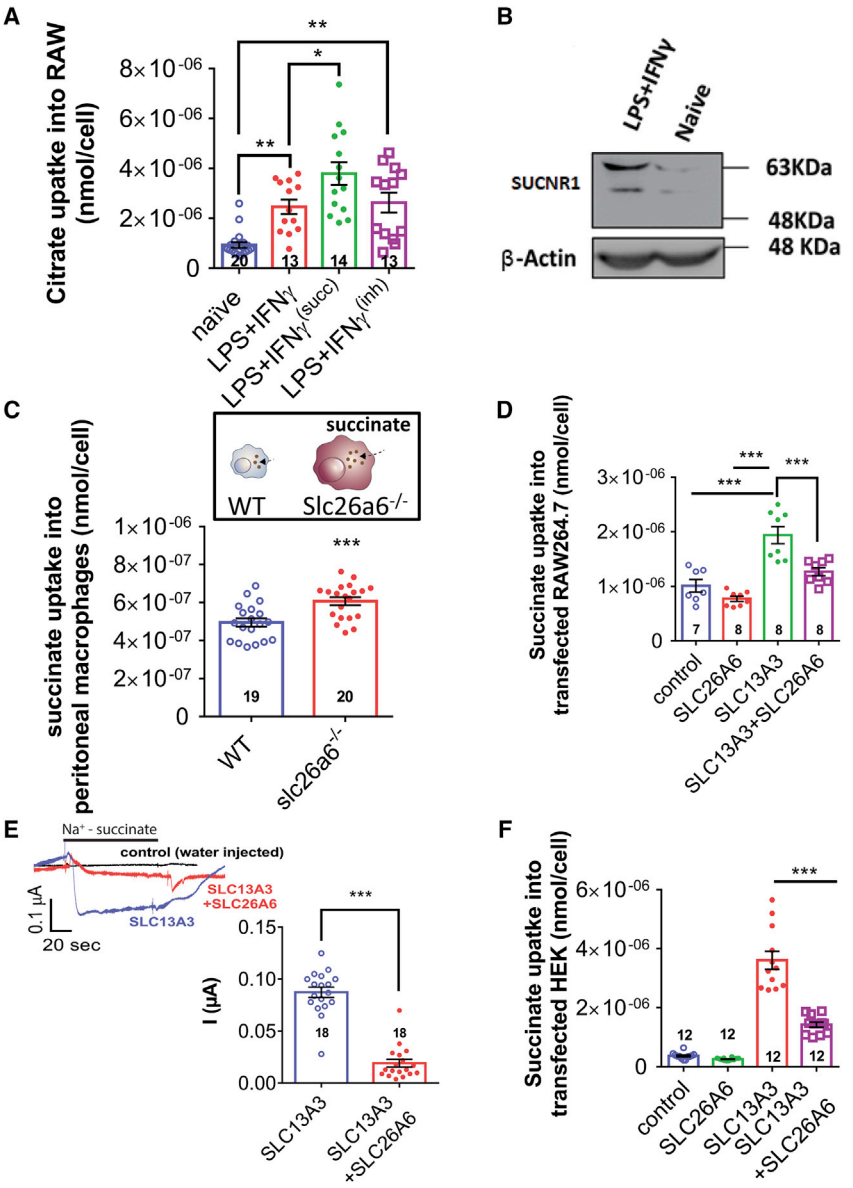


**Figure 2. The Na$^+$-dependent succinate uptake by macrophages is likely mediated by an SLC13 transporter and regulated by SUCNR1 and SLC26A6**

(A) Citrate uptake was measured in either naive- or LPS/IFNγ-treated RAW264.7 cells. Notably, the SLC13A5 inhibitor (inh) did not affect citrate uptake, which was increased by application of 250 μM succinate (succ), potentially because of stimulation of SUCNR1, which is significantly elevated in LPS/IFNγ-treated cells.

(B) Western blot analysis of SUCNR1 expression in either naive or LPS/IFNγ-treated RAW264.7 macrophages.

(C) The uptake of succinate was monitored using a radiolabeled succinate flux assay in peritoneal macrophages that were isolated from either WT or SLC26A6$^{-/-}$ mice.

(D–F) The regulatory effect of SLC26A6 on SLC13A3-mediated succinate uptake monitored in RAW264.7 cells (D) in *Xenopus* oocytes (E) or in HEK293 cells (F) expressing SLC13A3 and SLC26A6, as indicated.

Data are shown as means ± SEM. Statistical significance was assessed with either t test or one-way ANOVA followed by Tukey's post-test. *p < 0.05, **p < 0.01, ***p < 0.001.

SLC13A5 does not play a major role in mediating Na$^+$-dependent succinate transport in macrophages. Previous studies have indicated that the Slc13a3 gene expression is highly regulated during mouse macrophage plasticity (Jablonski et al., 2015). These findings suggest that SLC13A3 may play a key role in mediating and regulating succinate transport in macrophages, yet the contribution of SLC13A2 cannot be ruled out.

Previously, the $Cl^-/HCO_3^-$/oxalate transporter, Slc26a6, which is expressed in macrophages (Figure S1E; Noubade et al., 2014), was shown to interact with SLC13 transporters to inhibit succinate uptake (Khamaysi et al., 2019, 2020; Ohana et al., 2013). As shown in Figure 2C, succinate uptake into peritoneal macrophages was ~20% higher in slc26a6$^{-/-}$ mice compared with wild-type (WT).

To test whether SLC26A6 regulates succinate uptake via SLC13A3, we expressed SLC13A3 and SLC26A6 either alone or together in RAW264.7 macrophages (Figure 2D) in *Xenopus* oocytes (Figure 2E), as well as in HEK293 cells (Figure 2F), and monitored succinate uptake and currents. In agreement with the results in Figure 2C, we found that SLC26A6 significantly inhibits SLC13A3 activity in all cells.

Jointly, our results in Figures 1 and 2 indicate that the Na$^+$-dependent uptake of succinate into pro-inflammatory macrophages is significantly elevated compared with either naive or anti-inflammatory polarized macrophages. In addition, SLC13A3-mediated succinate uptake and its regulation by SUCNR1 or SLC26A6 perpetuate the pro-inflammatory state of macrophages by elevating cytoplasmic succinate concentrations (Figure 1F).

## The intestinal tissue mediates Na$^+$-dependent succinate uptake to control succinate delivery to macrophages

In the gut, transepithelial succinate absorption is mediated by the SLC13 family of succinate transporters, most notably, the apical transporters, SLC13A2 and SLC13A5, as well as the basolateral transporter, SLC13A3 (Markovich and Murer, 2004; Pajor, 2006). These members of the SLC13 family of transporters mediate Na$^+$-dependent succinate and citrate transport. To demonstrate the pivotal role of SLC13 transporters in mediating transepithelial succinate absorption, we monitored

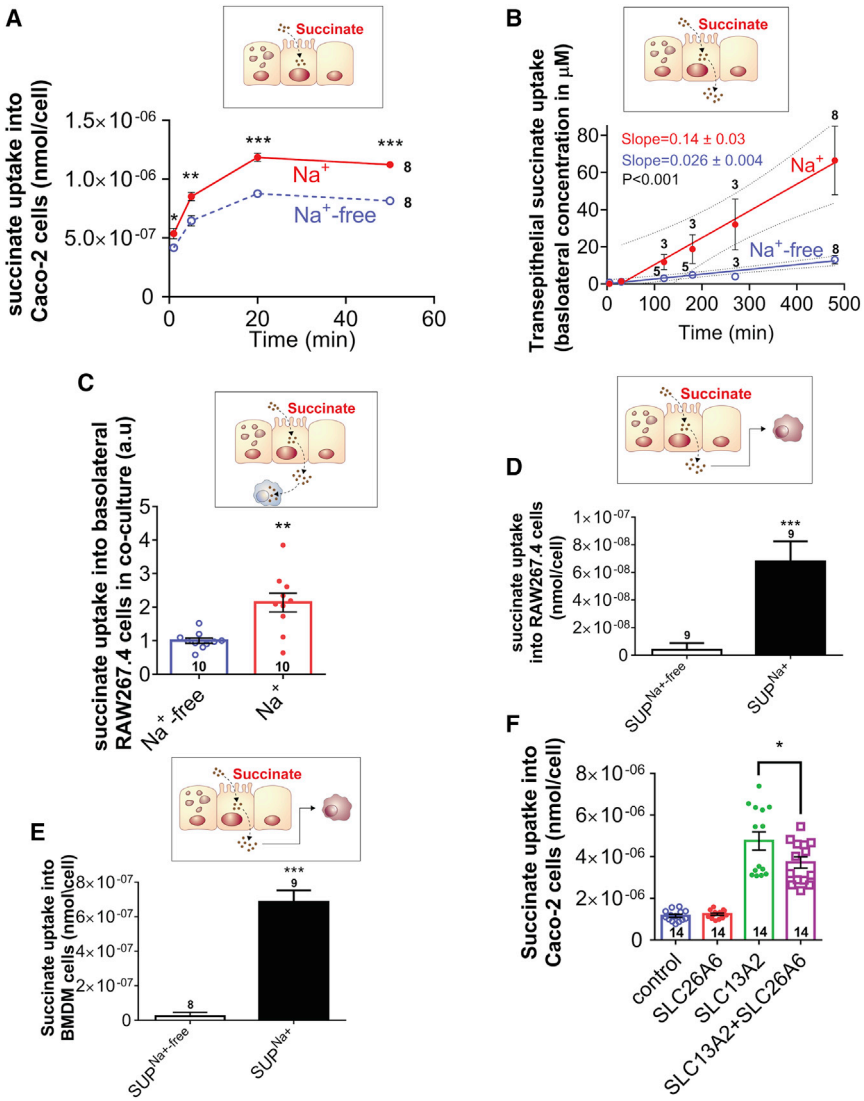


**Figure 3. Transepithelial succinate absorption and delivery to macrophages are $Na^+$ dependent**

(A) $^{14}$C-succinate uptake into Caco-2 monolayer is significantly elevated in the presence of 1 mM succinate and extracellular $Na^+$, suggesting slc13 transporter-mediated influx.

(B) Transepithelial transport rates via Caco-2 cell Transwell monolayer are dramatically elevated in the presence of extracellular $Na^+$.

(C) Succinate was administered to the apical chamber of a Caco-2 monolayer Transwell culture in the presence or absence of $Na^+$, and succinate concentrations were monitored in macrophages that were co-cultured at the basolateral chamber.

(D and E) In addition, the basolateral media were collected and added to separately cultured LPS/IFNγ-treated RAW264.7 macrophages (D) or BMDMs (E) to measure succinate uptake.

(F) Caco-2 cells were transfected with either SLC13A2 or SLC26A6, as indicated, and succinate uptake was monitored.

Data are shown as means ± SEM. Statistical significance was assessed either with t test or one-way ANOVA followed by Tukey's post-test. *p < 0.05, **p < 0.01, ***p < 0.001.

succinate uptake into a monolayer of a human intestinal cell line (Caco-2) that was shown to express specific SLC13s (Weerachayaphorn and Pajor, 2008). As shown in Figure 3A, we monitored a time-dependent increase in succinate uptake into the epithelial cells in the presence of sodium compared with its absence, suggesting that SLC13 members mediate succinate influx in the human intestinal epithelial cells. To determine transepithelial uptake of succinate, we utilized a culture of Caco-2 cells monolayer in Transwell inserts. We applied succinate in the presence of $^{14}$C-succinate to the apical chamber and monitored succinate concentrations at the basolateral chamber (as described in the STAR Methods). As shown in Figure 3B, the transepithelial succinate uptake rate is increased about 5.4-fold in the presence of $Na^+$. Next, we co-cultured Caco-2 (apical) and LPS/IFNγ-treated macrophages (basolateral) in a Transwell system, applied succinate to the apical chamber, and monitored succinate uptake into the basolateral macrophages (Figure 3C). In addition, we collected the basolateral media and applied it to LPS/IFNγ-treated RAW264.7 (Figure 3D) and BMDMs (Figure 3E) cultured separately. Our results suggest that transepithelial succinate uptake and basolateral succinate concentrations are significantly higher in the presence of $Na^+$ compared with those in the absence of $Na^+$. Consequently, succinate uptake into LPS/IFNγ-treated macrophages, which reside in the basolateral side, is also higher (Figure 3C). Finally, we transfected Caco-2 cells with SLC13A2, SLC26A6, or SLC13A2 and SLC26A6 together; monitored succinate uptake (Figure 3F); and found that SLC26A6 inhibits the SLC13A2-mediated succinate uptake.

Together, our results from the gut epithelia-macrophages model system indicate that epithelial succinate transporters mediate succinate delivery to macrophages from the gut lumen, as well as succinate uptake by macrophages, to modulate inflammation.

## The gene expression of proteins that inhibit epithelial succinate uptake and facilitate succinate clearance is upregulated in IBDs

In epithelia, the SLC26 transporters, SLC26A3 and SLC26A6, as well as SUCNR1 stimulation, inhibit succinate uptake, while the basolateral SLC13A3 mediates succinate clearance (Khamaysi et al., 2019; Ohana et al., 2013). Remarkably, genetic variation in SLC26A3 was associated with IBD and UC in genome-wide association studies (GWASs) (Asano et al., 2009; Liu et al., 2015). To begin assessing the contribution of

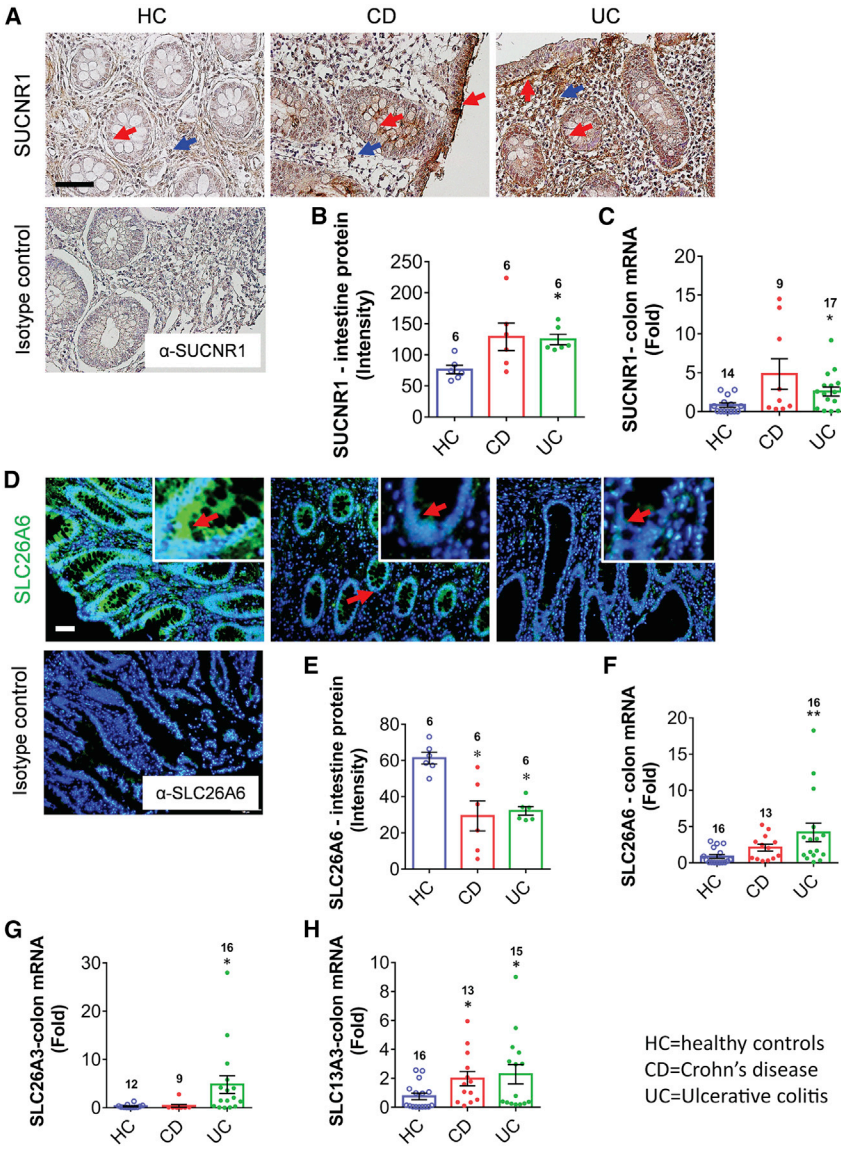


**Figure 4. The expression of determinants that either inhibit succinate uptake or mediate succinate clearance in intestinal and colon tissues of IBD patients**

(A and B) Representative images of immunohistochemistry analysis (A) and summary (B) of SUCNR1 protein expression in the intestine of either healthy conrol (HC), Crohn's disease (CD), or ulcerative colitis (UC) patients. SUCNR1 expression was detected in epithelial cells and in the lamina propria (arrows).

(C) The gene expression of SUCNR1 in colon tissues of HCs, CD patients, or UC patients.

(D and E) Representative images of immunofluorescence analysis (D) and summary (E) of SLC26A6 protein expression (green) in the intestine of HCs, CD patients, or UC patients. SLC26A6 expression was mainly detected in epithelial cells (arrows). Red arrows and blue arrows indicate the apical side of epithelial cells and macrophages, respectively. Nuclei were counterstained with DAPI (blue).

(F–H) The gene expression of SLC26A6 (F), SLC26A3 (G), and SLC13A3 (H) was monitored in colon tissues of HCs, CD patients, or UC patients, as indicated. The transcript levels were quantified by real-time qRT-PCR.

Data are shown as means ± SEM. Statistical significance was assessed using one-way ANOVA Kruskal-Wallis test followed by Dunn's post-test. *$p < 0.05$, **$p < 0.01$.

disturbed succinate homeostasis in IBD, we monitored protein and gene expression of transporters that control succinate homeostasis in intestinal and colon tissue biopsies from either healthy control subjects (HCs), CD patients, or UC patients (Figure 4). We found that the gene expression of SUCNR1 (Figures 4A–4C) was upregulated in the intestine and whole colon of patients with CD and UC, as indicated. However, although protein expression of SLC26A6 in the intestine is reduced in UC and CD patients (Figures 4D and 4E), the gene expression of SLC26A6 in the colon was elevated (Figure 4F). We also monitored the gene expression of SLC26A3 (Figure 4G) and SLC13A3 (Figure 4H). We found that both genes were upregulated in the colon of patients with CD and UC, with the exception of SLC26A3 expression that was changed in UC only, in agreement with the GWAS. This indicates that in our cohort of IBD patients, the gut tissue expression of genes, which encode for proteins that function to lower succinate absorption and elevate succinate clearance, is increased, most likely as a protective mechanism to prevent the excessive surge of the pro-inflammatory succinate.

## Succinate is elevated in the feces and serum of IBD patients and in samples from an IBD mouse model

To test whether the impaired epithelial succinate transport pathway fails to control succinate homeostasis in IBD, we collected serum from HCs and from patients with CD or UC and measured succinate concentrations. We found that serum succinate concentrations were significantly increased in patients with either CD or UC (Figure 5A). To identify whether the elevated serum succinate originates from an increase of succinate in the gut, we measured succinate concentrations in human and mouse fecal biospecimens collected from either IBD patients or mice with dextran sulfate sodium (DSS)-induced colitis and compared those with HCs. Indeed, the succinate levels were significantly increased in the feces of IBD patients (Figure 5B) and mice with DSS-induced colitis (Figure 5C) compared with controls. These findings suggest that in IBD, the gut tissue is exposed to high levels of succinate in the lumen and circulation. This may stem from lower SLC26A6 expression in the intestine (Figure 4D and 4E), because SLC26A6 inhibits SLC13A2-mediated succinate transport in epithelial cells (Figure 3F). Yet,

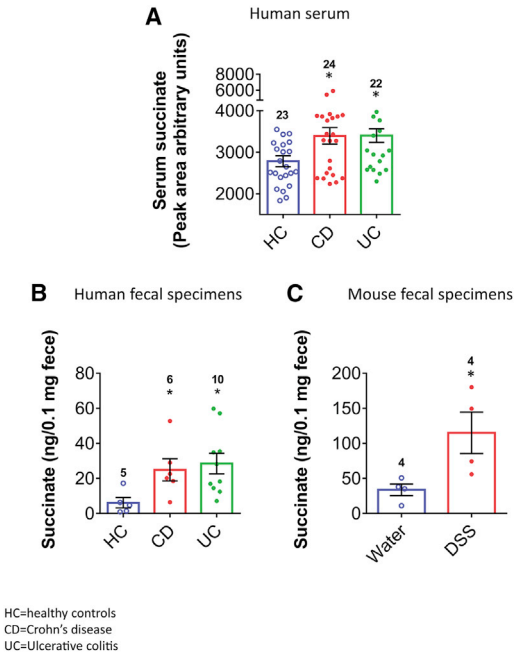


**Figure 5. Succinate concentrations are elevated in the serum and fecal specimens of IBD patients and a mouse model of UC**

We measured succinate concentrations in the serum of human samples using gas chromatography time-of-flight mass spectrometry (GC-TOF-MS),variable importance plot (VIP) > 1.0.

(A) Panel depicts the mean and distribution of serum succinate levels in either CD or UC. Data are shown as means ± SEM. *p < 0.05.

(B and C) In addition, we monitored fecal succinate concentrations in human samples (B) and in mouse samples (C).

Data are shown as means ± SEM. Statistical significance was assessed either using t test for two-group comparison or using one-way ANOVA followed by multiple comparison test. *p < 0.05. DSS, treated with 2.5% dextran sodium sulfate.

elevated expression of other genes and proteins that protect from the succinate surge (Figure 4) fails to prevent elevated succinate absorption.

### The microbiota of UC patients and the mouse model are enriched with succinate-producing bacteria and impoverished of succinate-consuming bacteria

Elevated succinate in IBD may be a result of changes in the composition of specific bacteria that metabolize succinate in the gut or increased invasion of these microbes into the gut wall. Hence we investigated the microbiome using 16S rRNA gene pyrosequencing of feces and colon tissues from HC and IBD patients. Beta-diversity (PCoA) and alpha-diversity (Shannon index, Chao1 index, and Simpson index) showed a distinct clustering in the microbiome of HCs and IBD patients (Figures S2A and S2B and statistical analysis in Figure S3, tables 1 and 2, respectively) and reduced diversity in IBD samples (Figures S2C and S2D), as previously reported (Sheehan et al., 2015). We also identified the distinct feature of IBD that indicated a lower abundance of *Firmicutes* and higher abundance of *Proteobacteria* and *Bacteroidetes* compared with HCs (Figures S2E and S2F). We tested the abundance of succinate-producing bacteria species and found that *B. fragilis* was significantly increased in colon tissues of UC patients compared with HCs (Figure 6A). Moreover, we observed high abundance of the major succinate producer, *B. vulgatus*, in the tissue of both DSS- and TNBS-treated mice (Figure 6B). Strikingly, the abundance of the succinate-consuming bacteria *P. succinatutens* was significantly decreased in the human tissue of CD patients (Figure 6C), and we measured a similar trend for the succinate consumer *P. faecium* (Figure S4). Markedly, we detected high abundance of succinate-consuming bacteria in only a few healthy individuals, while the abundance of these bacteria in all IBD patients was either negligible or undetectable. The abundance of other succinate-producing/consuming bacterial species was not significantly changed in either CD tissue samples or fecal samples of IBD patients and mice compared with HCs (Figures S4 and S5). Other minor succinate-consuming bacteria, such as *Odoribacteraceae* and *Clostridiaceae*, were not observed in any group.

Together, our data suggest that the microbiota, which infiltrate the gut wall, are likely a major source for excessive succinate. High succinate is mainly influenced by elevated succinate production but may also be affected by diminished succinate consumption or a combination of both. This may lead to high succinate absorption in IBD patients and mouse models.

## DISCUSSION

Succinate was associated with increased invasion of bacteria into the host tissue that alters bacterial virulence in IBD (Zaidi et al., 2020) and in *Salmonella* infection (Rosenberg et al., 2021). The gut commensals may often invade the host gut tissue and trigger an immune response that involves the activation of innate immune cells, such as dendritic cells, macrophages, and neutrophils, to effectively kill the microbes. An excessive immune response may result in tissue damage, yet a healthy gut is capable of regenerating a normal and tight barrier. Nevertheless, genetic or environmental factors hamper the barrier regeneration in IBD patients, which might stem from local activation of intense immune responses triggered by either immune cells or epithelial cells that secrete pro-inflammatory cytokines (Garcia-Carbonell et al., 2019; Neurath, 2019; Schoultz and Keita, 2019). Importantly, metabolic changes and particularly elevated cytoplasmic succinate stimulate pro-inflammatory cytokine secretion. It is therefore conceivable that continuous elevation of succinate levels by commensals, pathogens, or host cells will trigger, sustain, or exacerbate a chronic inflammatory response. Here, we found that transepithelial delivery of succinate to macrophages is mediated by the SLC13 transporters and regulated by SLC26 transporters in epithelial cells and macrophages (Figures 1, 2, and 3). Consequently, we show that succinate uptake leads to a significant and time-dependent elevation in NO secretion by macrophages that were stimulated with LPS and IFNγ. Importantly, the effect of extracellular succinate uptake on NO secretion was monitored in the absence of L-glutamine in the media to attenuate intracellular succinate production. The perpetuation of the pro-inflammatory state in macrophages may occur because of elevation of cytoplasmic succinate that stabilizes HIF (Tannahill et al., 2013).

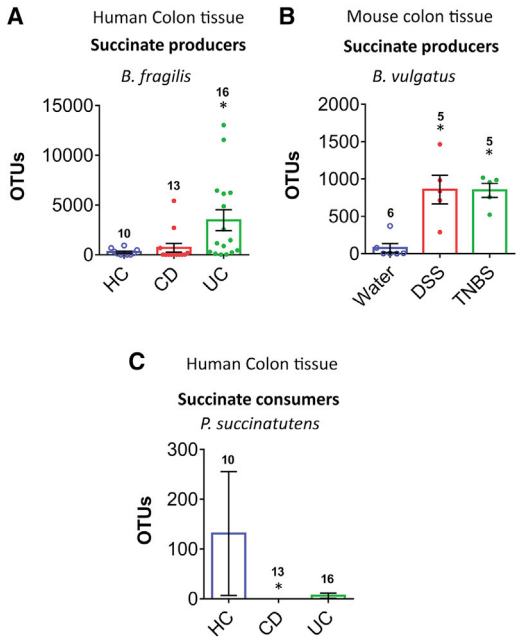


**Figure 6. The abundance of succinate-metabolizing bacteria in the colon tissue is disrupted in patients with IBD and in a colitis mouse model**

(A–C) We assessed succinate-producing bacteria (A and B) and succinate-consuming bacteria (C) in colon tissues using metagenome analysis at the species level in either IBD patients (A and C) or colitis mouse models (DSS- and TNBS-treated) (B) compared with HCs.

Data are shown as means ± SEM. The data were analyzed using one-way ANOVA followed by a multiple comparisons post-test. *$p < 0.05$. DSS, treated with dextran sodium sulfate; OTUs, operational taxonomic units; TNBS, treated with trinitrobenzene sulfonic acid.

Most notably, several IBD-associated extraintestinal pathologies were implicated with elevated succinate concentrations, namely, arthritis (Littlewood-Evans et al., 2016) and calcium-oxalate kidney stones (Khamaysi et al., 2019; Ohana et al., 2013). Interestingly, some extraintestinal pathologies were identified in IBD patients prior to the onset of the gut symptoms (Arvikar and Fisher, 2011). These observations suggest that although IBDs are characterized by intense immune responses, the underlying cause may not be immunological in nature. Therefore, we argue that IBD may be a significant symptom of a broad metabolic syndrome of hampered succinate homeostasis. An immediate question that arises is: why does the intestine actively absorb the pro-inflammatory succinate under physiological conditions? One plausible answer to this question was provided by De Vadder et al. (2016), who show that normal levels of microbiota-produced succinate are necessary to improve glucose homeostasis by gluconeogenesis that takes place in the intestinal epithelia. Here, we measured succinate concentrations in IBD patients, as well as mouse models, and found that in IBD, succinate is significantly elevated in the feces and the serum (Figure 5). These findings may suggest that high luminal succinate in the intestine of IBD patients leads to elevated absorption of succinate. This is further supported by a previous study, which reported elevated fecal succinate concentrations in human IBD patients (Hallert et al., 2003) and in an IBD mouse model (Ariake et al., 2000; Osaka et al., 2017). High serum succinate levels were also found in obese individuals (Serena et al., 2018). Intriguingly, obesity is strongly associated with IBD because 15%–40% of IBD patients are obese (Singh et al., 2017).

Importantly, we also found that the gene expression of SUCNR1, SLC26A6, SLC26A3, and SLC13A3 were elevated in the colon of IBD patients (Figures 4C and 4F–4H). These genes encode proteins that act to lower succinate absorption by regulating apical uptake (SLC26A3, SLC26A6, SUCNR1) or mediating basolateral clearance (SLC13A3). As we show here, SLC13A3, SLC26A6 (Figures 2C and 2D), and SUCNR1 (Figure 2A) may also regulate succinate transport in macrophages. Notably, a strong association was reported in a genome-wide association IBD study with the SLC26A3 gene (Asano et al., 2009; Liu et al., 2015). Therefore, in our cohort, the observed up-regulation of these genes is likely a protective measure to lower the pathological succinate surge in the colon. In contrast, if the expression of proteins that regulate succinate transporters is lowered, as suggested for SLC26A3 in several reports (reviewed here and by Priyamvada et al., 2015), this may elevate the uptake of succinate and exacerbate inflammation. In our cohort, we found that although the protein expression of SUCNR1 is elevated (Figures 4A and 4B), the expression of SLC26A6 was lower in the intestine of IBD patients (Figures 4D and 4E). Low SLC26A6 expression is expected to reduce the inhibition of succinate uptake by SLC13 transporters and, thus, elevate transepithelial succinate absorption leading to high serum succinate (Figure 5A). Taken together, our results and previous studies indicate that changes in the expression of succinate transport regulating proteins in IBD patients may vary between individuals, populations, and maybe also during the course of the disease, but they ultimately lead to elevated succinate flux and inflammation.

Other metabolites were also implicated with immune response regulation. For example, the signaling of short-chain fatty acids (SCFAs), such as acetate, butyrate, and propionate, via GPR41 and GPR43, as well as other metabolite receptors, show significant anti-inflammatory effects (Tan et al., 2017). This suggests that the balance between succinate and SCFAs or other metabolites may modulate inflammatory processes. It is, therefore, not surprising that the diet and microbiota composition play a key role in inflammation. Several bacterial species produce SCFAs through fermentation of dietary fibers, where succinate is a product of the microbial metabolic pathway of the SCFA, propionate, as reported for *B. fragilis* (Macy et al., 1978). Remarkably, the most significant dysbiosis we found in our metagenomic analysis was the elevation of *B. fragilis* in the tissue of UC patients (Figure 6A). Several bacteria, including *B. fragilis*, were known as typical microorganisms used for fermentative succinate production (Cao et al., 2013). It was shown that reconstitution of microbiota-depleted mice with the succinate-producing commensal, *B. thetaiotaomicron*, augmented GI pathophysiology during *C. rodentium* infection, enhancing edema of the colonic epithelium, exacerbating crypt destruction, increasing immune infiltration, and impairing intestinal epithelial repair (Connors et al., 2018; Curtis et al., 2014). Nevertheless, numerous studies suggest that significant

variance occurs in the dysbiosis pattern between different IBD patient populations (Ni et al., 2017). Clearly, there is also a very high variance in gene expression between different IBD populations (Jostins et al., 2012; Liu et al., 2015). Our findings suggest that the pathology is not a result of a specific gene expression pattern or the microbiota population, but rather the manifestation of the metabolite composition in the gut. In other words, different microbiota compositions can generate high succinate concentrations that either cause or maintain IBD. For example, high abundance of succinate-producing bacteria or, alternatively, low abundance of succinate-consuming bacteria is expected to elevate mucosal succinate concentration. Indeed, a previous metagenomic analysis reported a reduced abundance of succinate-consuming *Phascolarctobacterium* among IBD patients (Morgan et al., 2012). Consistent with this, we now show a decreased abundance of the succinate-consuming bacteria *P. succinatutens* in CD patients (Figure 6C). This may explain the high fecal succinate we monitored in IBD (Figures 5B and 5C) and the lack of significant increase in the abundance of succinate-producing bacteria in our cohort's CD patients (Figure 6A; Figures S4 and S5). Subsequently, as we show here, the transport and signaling pathways on both epithelial cells and macrophages are required to modulate succinate homeostasis. Any impairment along these pathways or a breach of the epithelial barrier can potentially increase succinate concentrations in the macrophages' extracellular or intracellular milieu, leading to chronic inflammation.

### Ethics approval

This study was approved by the Institutional Review Board of Severance Hospital, Yonsei University (4-2012-0302). Patient consent was obtained.

### Limitations of the study

In this study, we have identified the role of specific transporters in mediating transepithelial succinate uptake and delivery into macrophages. We also found that determinants within this system and succinate-metabolizing microbiota are significantly altered during IBD. Nevertheless, the function of SUCNR1, SLC13 transporters, and SLC26 transporters requires further characterization to determine their precise role in mediating and regulating succinate homeostasis in macrophages. These open questions should be addressed in future studies using *in vitro* and *in vivo* systems to determine how impaired function of succinate signaling and transport systems is associated with IBD and, potentially, other comorbidities and inflammatory diseases.

## STAR★METHODS

Detailed methods are provided in the online version of this paper and include the following:

- KEY RESOURCES TABLE
- RESOURCE AVAILABILITY
  - Lead contact
  - Materials availability
  - Data and code availability
- EXPERIMENTAL MODEL AND SUBJECT DETAILS
  - Human volunteers
  - Animal models
  - Cell cultures and transwell® system
  - Bone marrow-derived and peritoneal macrophages
- METHOD DETAILS
  - Succinate assay of fecal samples
  - Succinate evaluation of serum samples
  - Evaluation of microbiota changes by pyrosequencing
  - Protein expression analysis by western blotting
  - Succinate and citrate uptake measurements
  - Preparation and injection of oocytes
  - Voltage and current measurement in oocytes
  - Immunohistochemistry and immunofluorescent staining
  - Quantitative real-time reverse-transcription polymerase chain reaction (qRT-PCR)
  - Flow Cytometry
  - Nitric Oxide (NO) quantification assay
- QUANTIFICATION AND STATISTICAL ANALYSIS

## SUPPLEMENTAL INFORMATION

Supplemental information can be found online at https://doi.org/10.1016/j.celrep.2021.109521.

## ACKNOWLEDGMENTS

This work was supported by BSF (grant no. 2015003 to E.O.), ISF (grant no. 271/16 and 2164/16 to E.O.), and Mid-career Researcher Program through NRF grant funded by the Korea government (MSIP) (NRF-2017R1A2B4001848 to J.H.C.). We thank Dr. Boris M. Baranovski and Ido Brami for their technical assistance with cell cultures and image preparation. We would also like to thank MID (Medical Illustration & Design) for providing support with medical illustrations.

## AUTHOR CONTRIBUTIONS

E.O. designed the study; M.F., S.W.K., A.K., L.S., H.E.-R., I.S.P., and U.H. performed experiments; E.O., M.F., A.K., and S.W.K. were involved in data analysis; sample acquisition was performed by J.H.C.; E.O. and J.H.C. were involved in funding acquisition; M.F., S.W.K., J.H.C., and E.O. wrote the manuscript. All authors contributed to critical revision of the manuscript and approved the final version.

## DECLARATION OF INTERESTS

The patent application "Succinate-Binding Polypeptides and Use Thereof" (PCT/IL2018/051060) by E.O. is related to this work.

Received: April 6, 2020
Revised: February 23, 2021
Accepted: July 21, 2021
Published: August 10, 2021

## REFERENCES

Amend, S.R., Valkenburg, K.C., and Pienta, K.J. (2016). Murine Hind Limb Long Bone Dissection and Bone Marrow Isolation. J. Vis. Exp. *2016*, 53936.

Ariake, K., Ohkusa, T., Sakurazawa, T., Kumagai, J., Eishi, Y., Hoshi, S., and Yajima, T. (2000). Roles of mucosal bacteria and succinic acid in colitis caused by dextran sulfate sodium in mice. J. Med. Dent. Sci. *47*, 233–241.

Arvikar, S.L., and Fisher, M.C. (2011). Inflammatory bowel disease associated arthropathy. Curr. Rev. Musculoskelet. Med. *4*, 123–131.

Asano, K., Matsushita, T., Umeno, J., Hosono, N., Takahashi, A., Kawaguchi, T., Matsumoto, T., Matsui, T., Kakuta, Y., Kinouchi, Y., et al. (2009). A genome-wide association study identifies three new susceptibility loci for ulcerative colitis in the Japanese population. Nat. Genet. *41*, 1325–1329.

Brami, I., Ini, D., Sassonker, N., Zaknoun, M., Zuckerman, T., and Lewis, E.C. (2020). Immunosuppressive Drugs Alter α1-Antitrypsin Production in Hepatocytes: Implications for Epithelial Gap Repair. Biol. Blood Marrow Transplant. *26*, 625–633.

Browne, J.L., Sanford, P.A., and Smyth, D.H. (1978). Transfer and metabolism of citrate, succinate, alpha-ketoglutarate and pyruvate by hamster small intestine. Proc. R. Soc. Lond. B Biol. Sci. *200*, 117–135.

Cao, Y., Zhang, R., Sun, C., Cheng, T., Liu, Y., and Xian, M. (2013). Fermentative succinate production: an emerging technology to replace the traditional petrochemical processes. BioMed Res. Int. *2013*, 723412.

Chun, J., Kim, K.Y., Lee, J.H., and Choi, Y. (2010). The analysis of oral microbial communities of wild-type and toll-like receptor 2-deficient mice using a 454 GS FLX Titanium pyrosequencer. BMC Microbiol. *10*, 101.

Colombel, J.F., Sandborn, W.J., Reinisch, W., Mantzaris, G.J., Kornbluth, A., Rachmilewitz, D., Lichtiger, S., D'Haens, G., Diamond, R.H., Broussard, D.L., et al.; SONIC Study Group (2010). Infliximab, azathioprine, or combination therapy for Crohn's disease. N. Engl. J. Med. *362*, 1383–1395.

Connors, J., Dawe, N., and Van Limbergen, J. (2018). The Role of Succinate in the Regulation of Intestinal Inflammation. Nutrients *11*, 25.

Curtis, M.M., Hu, Z., Klimko, C., Narayanan, S., Deberardinis, R., and Sperandio, V. (2014). The gut commensal Bacteroides thetaiotaomicron exacerbates enteric infection through modification of the metabolic landscape. Cell Host Microbe *16*, 759–769.

De Minicis, S., Seki, E., Uchinami, H., Kluwe, J., Zhang, Y., Brenner, D.A., and Schwabe, R.F. (2007). Gene expression profiles during hepatic stellate cell activation in culture and in vivo. Gastroenterology *132*, 1937–1946.

De Vadder, F., Kovatcheva-Datchary, P., Zitoun, C., Duchampt, A., Bäckhed, F., and Mithieux, G. (2016). Microbiota-Produced Succinate Improves Glucose Homeostasis via Intestinal Gluconeogenesis. Cell Metab. *24*, 151–157.

DeGruttola, A.K., Low, D., Mizoguchi, A., and Mizoguchi, E. (2016). Current Understanding of Dysbiosis in Disease in Human and Animal Models. Inflamm. Bowel Dis. *22*, 1137–1150.

Emami Riedmaier, A., Nies, A.T., Schaeffeler, E., and Schwab, M. (2012). Organic anion transporters and their implications in pharmacotherapy. Pharmacol. Rev. *64*, 421–449.

Garcia-Carbonell, R., Yao, S.J., Das, S., and Guma, M. (2019). Dysregulation of Intestinal Epithelial Cell RIPK Pathways Promotes Chronic Inflammation in the IBD Gut. Front. Immunol. *10*, 1094.

Hallert, C., Björck, I., Nyman, M., Pousette, A., Grännö, C., and Svensson, H. (2003). Increasing fecal butyrate in ulcerative colitis patients by diet: controlled pilot study. Inflamm. Bowel Dis. *9*, 116–121.

Higuchi, K., Kopel, J.J., Sivaprakasam, S., Jaramillo-Martinez, V., Sutton, R.B., Urbatsch, I.L., and Ganapathy, V. (2020). Functional analysis of a species-specific inhibitor selective for human Na+-coupled citrate transporter (NaCT/SLC13A5/mINDY). Biochem. J. *477*, 4149–4165.

Hong, J.H., Yang, D., Shcheynikov, N., Ohana, E., Shin, D.M., and Muallem, S. (2013). Convergence of IRBIT, phosphatidylinositol (4,5) bisphosphate, and WNK/SPAK kinases in regulation of the Na+-HCO3- cotransporters family. Proc. Natl. Acad. Sci. USA *110*, 4105–4110.

Jablonski, K.A., Amici, S.A., Webb, L.M., Ruiz-Rosado, Jde.D., Popovich, P.G., Partida-Sanchez, S., and Guerau-de-Arellano, M. (2015). Novel Markers to Delineate Murine M1 and M2 Macrophages. PLoS ONE *10*, e0145342.

Jostins, L., Ripke, S., Weersma, R.K., Duerr, R.H., McGovern, D.P., Hui, K.Y., Lee, J.C., Schumm, L.P., Sharma, Y., Anderson, C.A., et al.; International IBD Genetics Consortium (IIBDGC) (2012). Host-microbe interactions have shaped the genetic architecture of inflammatory bowel disease. Nature *491*, 119–124.

Keiran, N., Ceperuelo-Mallafré, V., Calvo, E., Hernández-Alvarez, M.I., Ejarque, M., Núñez-Roa, C., Horrillo, D., Maymó-Masip, E., Rodríguez, M.M., Fradera, R., et al. (2019). SUCNR1 controls an anti-inflammatory program in macrophages to regulate the metabolic response to obesity. Nat. Immunol. *20*, 581–592.

Khamaysi, A., Anbtawee-Jomaa, S., Fremder, M., Eini-Rider, H., Shimshilashvili, L., Aharon, S., Aizenshtein, E., Shlomi, T., Noguchi, A., Springer, D., et al. (2019). Systemic succinate homeostasis and local succinate signaling affect blood pressure and modify risks for calcium oxalate lithogenesis. J. Am. Soc. Nephrol. *30*, 381–392.

Khamaysi, A., Aharon, S., Eini-Rider, H., and Ohana, E. (2020). A dynamic anchor domain in slc13 transporters controls metabolite transport. J. Biol. Chem. *295*, 8155–8163.

Kim, D.H., Kim, S., Lee, J.H., Kim, J.H., Che, X., Ma, H.W., Seo, D.H., Kim, T.I., Kim, W.H., Kim, S.W., and Cheon, J.H. (2019). Lactobacillus acidophilus suppresses intestinal inflammation by inhibiting endoplasmic reticulum stress. J. Gastroenterol. Hepatol. *34*, 178–185.

Kojima, R., Sekine, T., Kawachi, M., Cha, S.H., Suzuki, Y., and Endou, H. (2002). Immunolocalization of multispecific organic anion transporters, OAT1, OAT2, and OAT3, in rat kidney. J. Am. Soc. Nephrol. *13*, 848–857.

Lei, W., Ren, W., Ohmoto, M., Urban, J.F., Jr., Matsumoto, I., Margolskee, R.F., and Jiang, P. (2018). Activation of intestinal tuft cell-expressed Sucnr1 triggers type 2 immunity in the mouse small intestine. Proc. Natl. Acad. Sci. USA *115*, 5552–5557.

Littlewood-Evans, A., Sarret, S., Apfel, V., Loesle, P., Dawson, J., Zhang, J., Muller, A., Tigani, B., Kneuer, R., Patel, S., et al. (2016). GPR91 senses extracellular succinate released from inflammatory macrophages and exacerbates rheumatoid arthritis. J. Exp. Med. *213*, 1655–1662.

Liu, J.Z., van Sommeren, S., Huang, H., Ng, S.C., Alberts, R., Takahashi, A., Ripke, S., Lee, J.C., Jostins, L., Shah, T., et al.; International Multiple Sclerosis Genetics Consortium; International IBD Genetics Consortium (2015). Association analyses identify 38 susceptibility loci for inflammatory bowel disease and highlight shared genetic risk across populations. Nat. Genet. *47*, 979–986.

Lungkaphin, A., Lewchalermwongse, B., and Chatsudthipong, V. (2006). Relative contribution of OAT1 and OAT3 transport activities in isolated perfused rabbit renal proximal tubules. Biochim. Biophys. Acta *1758*, 789–795.

Macias-Ceja, D.C., Ortiz-Masiá, D., Salvador, P., Gisbert-Ferrándiz, L., Hernández, C., Hausmann, M., Rogler, G., Esplugues, J.V., Hinojosa, J., Alós, R., et al. (2019). Succinate receptor mediates intestinal inflammation and fibrosis. Mucosal Immunol. *12*, 178–187.

Macy, J.M., Ljungdahl, L.G., and Gottschalk, G. (1978). Pathway of succinate and propionate formation in Bacteroides fragilis. J. Bacteriol. *134*, 84–91.

Markovich, D., and Murer, H. (2004). The SLC13 gene family of sodium sulphate/carboxylate cotransporters. Pflugers Arch. *447*, 594–602.

Morgan, X.C., Tickle, T.L., Sokol, H., Gevers, D., Devaney, K.L., Ward, D.V., Reyes, J.A., Shah, S.A., LeLeiko, N., Snapper, S.B., et al. (2012). Dysfunction of the intestinal microbiome in inflammatory bowel disease and treatment. Genome Biol. *13*, R79.

Neurath, M.F. (2019). Targeting immune cell circuits and trafficking in inflammatory bowel disease. Nat. Immunol. *20*, 970–979.

Ni, J., Wu, G.D., Albenberg, L., and Tomov, V.T. (2017). Gut microbiota and IBD: causation or correlation? Nat. Rev. Gastroenterol. Hepatol. *14*, 573–584.

Nielsen, O.H., and Ainsworth, M.A. (2013). Tumor necrosis factor inhibitors for inflammatory bowel disease. N. Engl. J. Med. *369*, 754–762.

Niess, J.H., and Adler, G. (2010). Enteric flora expands gut lamina propria CX3CR1+ dendritic cells supporting inflammatory immune responses under normal and inflammatory conditions. J. Immunol. *184*, 2026–2037.

Niess, J.H., Brand, S., Gu, X., Landsman, L., Jung, S., McCormick, B.A., Vyas, J.M., Boes, M., Ploegh, H.L., Fox, J.G., et al. (2005). CX3CR1-mediated dendritic cell access to the intestinal lumen and bacterial clearance. Science *307*, 254–258.

Nikolaus, S., and Schreiber, S. (2007). Diagnostics of inflammatory bowel disease. Gastroenterology *133*, 1670–1689.

Noubade, R., Wong, K., Ota, N., Rutz, S., Eidenschenk, C., Valdez, P.A., Ding, J., Peng, I., Sebrell, A., Caplazi, P., et al. (2014). NRROS negatively regulates reactive oxygen species during host defence and autoimmunity. Nature *509*, 235–239.

Ohana, E., Shcheynikov, N., Moe, O.W., and Muallem, S. (2013). SLC26A6 and NaDC-1 transporters interact to regulate oxalate and citrate homeostasis. J. Am. Soc. Nephrol. *24*, 1617–1626.

Onizawa, M., Nagaishi, T., Kanai, T., Nagano, K., Oshima, S., Nemoto, Y., Yoshioka, A., Totsuka, T., Okamoto, R., Nakamura, T., et al. (2009). Signaling pathway via TNF-alpha/NF-kappaB in intestinal epithelial cells may be directly involved in colitis-associated carcinogenesis. Am. J. Physiol. Gastrointest. Liver Physiol. *296*, G850–G859.

Osaka, T., Moriyama, E., Arai, S., Date, Y., Yagi, J., Kikuchi, J., and Tsuneda, S. (2017). Meta-Analysis of Fecal Microbiota and Metabolites in Experimental Colitic Mice during the Inflammatory and Healing Phases. Nutrients *9*, 1329.

Pajor, A.M. (1995). Sequence and functional characterization of a renal sodium/dicarboxylate cotransporter. J. Biol. Chem. *270*, 5779–5785.

Pajor, A.M. (2006). Molecular properties of the SLC13 family of dicarboxylate and sulfate transporters. Pflugers Arch. *451*, 597–605.

Peruzzotti-Jametti, L., Bernstock, J.D., Vicario, N., Costa, A.S.H., Kwok, C.K., Leonardi, T., Booty, L.M., Bicci, I., Balzarotti, B., Volpe, G., et al. (2018). Macrophage-Derived Extracellular Succinate Licenses Neural Stem Cells to Suppress Chronic Neuroinflammation. Cell Stem Cell *22*, 355–368.e13.

Plevy, S.E., Landers, C.J., Prehn, J., Carramanzana, N.M., Deem, R.L., Shealy, D., and Targan, S.R. (1997). A role for TNF-alpha and mucosal T helper-1 cytokines in the pathogenesis of Crohn's disease. J. Immunol. *159*, 6276–6282.

Priyamvada, S., Gomes, R., Gill, R.K., Saksena, S., Alrefai, W.A., and Dudeja, P.K. (2015). Mechanisms Underlying Dysregulation of Electrolyte Absorption in Inflammatory Bowel Disease-Associated Diarrhea. Inflamm. Bowel Dis. *21*, 2926–2935.

Rosenberg, G., Yehezkel, D., Hoffman, D., Mattioli, C.C., Fremder, M., Ben-Arosh, H., Vainman, L., Nissani, N., Hen-Avivi, S., Brenner, S., et al. (2021). Host succinate is an activation signal for *Salmonella* virulence during intracellular infection. Science *371*, 400–405.

Rubic, T., Lametschwandtner, G., Jost, S., Hinteregger, S., Kund, J., Carballido-Perrig, N., Schwärzler, C., Junt, T., Voshol, H., Meingassner, J.G., et al. (2008). Triggering the succinate receptor GPR91 on dendritic cells enhances immunity. Nat. Immunol. *9*, 1261–1269.

Schmitz, H., Fromm, M., Bentzel, C.J., Scholz, P., Detjen, K., Mankertz, J., Bode, H., Epple, H.J., Riecken, E.O., and Schulzke, J.D. (1999). Tumor necrosis factor-alpha (TNFalpha) regulates the epithelial barrier in the human intestinal cell line HT-29/B6. J. Cell Sci. *112*, 137–146.

Schoultz, I., and Keita, A.V. (2019). Cellular and Molecular Therapeutic Targets in Inflammatory Bowel Disease-Focusing on Intestinal Barrier Function. Cells *8*, 193.

Schuster, R., Motola-Kalay, N., Baranovski, B.M., Bar, L., Tov, N., Stein, M., Lewis, E.C., Ayalon, M., and Sagiv, Y. (2020). Distinct anti-inflammatory properties of alpha1-antitrypsin and corticosteroids reveal unique underlying mechanisms of action. Cell. Immunol. *356*, 104177.

Seo, H., Oh, J., Hahn, D., Kwon, C.S., Lee, J.S., and Kim, J.S. (2017). Protective Effect of Glyceollins in a Mouse Model of Dextran Sulfate Sodium-Induced Colitis. J. Med. Food *20*, 1055–1062.

Serena, C., Ceperuelo-Mallafré, V., Keiran, N., Queipo-Ortuño, M.I., Bernal, R., Gomez-Huelgas, R., Urpi-Sarda, M., Sabater, M., Pérez-Brocal, V., Andrés-Lacueva, C., et al. (2018). Elevated circulating levels of succinate in human obesity are linked to specific gut microbiota. ISME J. *12*, 1642–1657.

Shcheynikov, N., Kim, K.H., Kim, K.M., Dorwart, M.R., Ko, S.B., Goto, H., Naruse, S., Thomas, P.J., and Muallem, S. (2004). Dynamic control of cystic fibrosis transmembrane conductance regulator Cl(-)/HCO3(-) selectivity by external Cl(-). J. Biol. Chem. *279*, 21857–21865.

Sheehan, D., Moran, C., and Shanahan, F. (2015). The microbiota in inflammatory bowel disease. J. Gastroenterol. *50*, 495–507.

Singh, S., Dulai, P.S., Zarrinpar, A., Ramamoorthy, S., and Sandborn, W.J. (2017). Obesity in IBD: epidemiology, pathogenesis, disease course and treatment outcomes. Nat. Rev. Gastroenterol. Hepatol. *14*, 110–121.

Smith, P.M., Howitt, M.R., Panikov, N., Michaud, M., Gallini, C.A., Bohlooly-Y, M., Glickman, J.N., and Garrett, W.S. (2013). The microbial metabolites, short-chain fatty acids, regulate colonic Treg cell homeostasis. Science *341*, 569–573.

Tan, J.K., McKenzie, C., Mariño, E., Macia, L., and Mackay, C.R. (2017). Metabolite-Sensing G Protein-Coupled Receptors-Facilitators of Diet-Related Immune Regulation. Annu. Rev. Immunol. *35*, 371–402.

Tannahill, G.M., Curtis, A.M., Adamik, J., Palsson-McDermott, E.M., McGettrick, A.F., Goel, G., Frezza, C., Bernard, N.J., Kelly, B., Foley, N.H., et al. (2013). Succinate is an inflammatory signal that induces IL-1β through HIF-1α. Nature *496*, 238–242.

Toma, I., Kang, J.J., Sipos, A., Vargas, S., Bansal, E., Hanner, F., Meer, E., and Peti-Peterdi, J. (2008). Succinate receptor GPR91 provides a direct link between high glucose levels and renin release in murine and rabbit kidney. J. Clin. Invest. *118*, 2526–2534.

Wang, L., and Sweet, D.H. (2013). Renal organic anion transporters (SLC22 family): expression, regulation, roles in toxicity, and impact on injury and disease. AAPS J. *15*, 53–69.

Wang, Y., Soyombo, A.A., Shcheynikov, N., Zeng, W., Dorwart, M., Marino, C.R., Thomas, P.J., and Muallem, S. (2006). Slc26a6 regulates CFTR activity in vivo to determine pancreatic duct HCO3- secretion: relevance to cystic fibrosis. EMBO J. *25*, 5049–5057.

Weerachayaphorn, J., and Pajor, A.M. (2008). Identification of transport pathways for citric acid cycle intermediates in the human colon carcinoma cell line, Caco-2. Biochim. Biophys. Acta *1778*, 1051–1059.

Zaidi, D., Huynh, H.Q., Carroll, M.W., Mandal, R., Wishart, D.S., and Wine, E. (2020). Gut Microenvironment and Bacterial Invasion in Paediatric Inflammatory Bowel Diseases. J. Pediatr. Gastroenterol. Nutr. *71*, 624–632.

## STAR★METHODS

### KEY RESOURCES TABLE

| REAGENT or RESOURCE | SOURCE | IDENTIFIERR |
|---|---|---|
| Antibodies | | |
| SUCNR1/GPR91 | Novusbio | Cat#NBP1-00861 |
| IL-1β | Santa Cruz Biotechnology | Cat#H-153 |
| donkey anti-goat IgG-HRP | Santa Cruz Biotechnology | Cat#Sc-2020 |
| CD206 | R&D Systems | Cat#AF2535 |
| Goat anti-Rabbit IgG (H+L) Cross-Adsorbed Secondary Antibody, HRP | Thermo Fisher | Cat#G21234 |
| β-Actin | Sigma-Aldrich | Cat#A3854 |
| F4/80 | Biogems | Cat#02922-80; Clone BM8.1 |
| CD16/CD32 | Biogems | Cat#08212; Clone 2.4G2 |
| CD11b | Biolegend | Cat#101215; Clone M1/70 |
| CD80 | Biolegend | Cat#104725; Clone 16-10A1 |
| SLC26A6 | Santa Cruz | Cat#sc-515230 |
| SUCNR1 | Abbexa | Cat#abx318542 |
| Goat anti-Mouse IgG (H+L) Cross-Adsorbed Secondary Antibody, Alexa Fluor 488 | Invitrogen | Cat#A-11001 |
| Goat Anti-Rabbit IgG Antibody (H+L), Biotinylated, R.T.U | VECTOR laboratories | Cat#BP-9100-50 |
| Biological samples | | |
| Human fecal samples, serum, gut tissues | Severance Hospital | N/A |
| Chemicals, peptides, and recombinant proteins | | |
| cOmplete, EDTA-free Protease Inhibitor Cocktail | Roche | Cat#11873580001 |
| Pierce Lane Marker Reducing Sample Buffer | Thermo Fisher Scientific | Cat#39000 |
| Citric acid | Sigma-Aldrich | Cat#C0759 |
| N-METHYL-D-GLUCAMINE | Sigma-Aldrich | Cat#M2004 |
| Sodium succinate | Sigma-Aldrich | Cat#14160 |
| Succinic acid | Sigma-Aldrich | Cat#S3674 |
| Dextran sulfate sodium (DSS) | MP Biomedicals | Cat#160110 |
| Chlorophenylalanine | Sigma-Aldrich | Cat#C6506 |
| 2,4,6-trinitrobenzene sulfonic acid (TNBS) | Thermo Fisher Scientific | Cat#28997 |
| Murine M-CSF | Peprotech | Cat#315-02 |
| IL-13 | Peprotech | Cat#210-13 |
| IL-4 | Peprotech | Cat#214-14 |
| IFNγ | Peprotech | Cat#315-05 |
| thioglycolate | Hylabs | Cat#TT137 |
| 70-μm strainer | FLACON | Cat#FAL352350 |
| LPS | Sigma-Aldrich | Cat#L2880 |
| 14C-Succinic acid | ViTrax Inc | Cat#VC 195 |
| 3H-Citric acid | ViTrax Inc | Cat#VT 295 |
| SLC13A5 inhibitor BI01383298 | TOCRIS Bioscience | CAS#2227549-00-8 |
| TRIzol | Thermo Fisher Scientific | Cat#15596018 |
| SYBR Green master mix | Thermo Fisher Scientific | Cat#4368708 |
| Horse serum | Vector | Cat#S-2000 |

(*Continued on next page*)

*Continued*

| REAGENT or RESOURCE | SOURCE | IDENTIFIERR |
|---|---|---|
| DMEM | Biological Industries | Cat#01-052-1A |
| L-Glutamine | Biological Industries | Cat#03-020-1B |
| Trypsin | Biological Industries | Cat#03-052-1B |
| FBS | Biological Industries | Cat#04-007-1A |
| Sodium pyruvate | Sigma-Aldrich | Cat#P5280 |
| PBS | Biological Industries | Cat#02-023-1A |
| **Critical commercial assays** | | |
| succinate Colorimetric Assay Kit | Sigma–Aldrich | Cat#MAK184 |
| cDNA Reverse Transcription Kit | Thermo Fisher Scientific | Cat#4368813 |
| Griess reagent system | Promega | Cat#G2930 |
| FastDNA SPIN Kit | MP Biomedicals | Cat#116560200 |
| **Deposited data** | | |
| microarray analysis data | Noubade et al., 2014 | GEO: GSE53986 |
| 16S rRNA Sequence identification | EzTaxon-e database | https://eztaxon-e.ezbiocloud.Net |
| **Experimental models: Cell lines** | | |
| RAW264.7 | Schuster et al., 2020 | N/A |
| C2BBe1 | Brami et al., 2020 | N/A |
| HEK293T | Khamaysi et al., 2019 | N/A |
| **Experimental models: Organisms/strains** | | |
| C57BL/6 mice | Orient, Seongnam, South Korea | N/A |
| C57BL/6 mice SLC26A6−/− | Gift from Prof. Shmuel Muallem; Wang et al., 2006; Ohana et al., 2013; Khamaysi et al., 2019 | N/A |
| *Xenopus laevis* | *Xenopus* One | N/A |
| **Oligonucleotides** | | |
| SLC26A6: forward 5′-CACCTCCCGGTTTTGGTCTG-3′ | Macrogen Inc | N/A |
| SLC26A6: reverse 5′-CAGGCCGGATAACAGGTCAC-3′ | Macrogen Inc | N/A |
| SLC26A3: forward 5′-AGATGCCCCACTACTCTGTCCT-3 | Macrogen Inc | N/A |
| SLC26A3: reverse 5′-ATCCACACCACACCTCTGCTT-3′ | Macrogen Inc | N/A |
| SLC13A3: forward 5′-CTTCATGCTCCCGGTCTCAAC-3′ | Macrogen Inc | N/A |
| SLC13A3: reverse 5′-GCCCAGGTATTCATAGCCAAA-3′ | Macrogen Inc | N/A |
| SUCNR1: forward 5′-GGAGACGTGCTCTGCATAAG-3′ | Macrogen Inc | N/A |
| SUCNR1: reverse 5′-AGGTGTTCTCGGAAAGGATACTT-3′ | Macrogen Inc | N/A |
| β-ACTIN: forward 5′-hCTCTTCCAGCCTTCCTTCCTG-3′ | Macrogen Inc | N/A |
| β-ACTIN: reverse 5′-CAGCACTGTGTTGGCGTACAG-3′ | Macrogen Inc | N/A |
| **Recombinant DNA** | | |
| Slc13a2 | Khamaysi et al., 2019 | RefSeq: BC096277 |
| Slc13a3 | Khamaysi et al., 2019 | RefSeq: BC026803 |
| Slc13a5 | Khamaysi et al., 2020 | RefSeq: BC143689 |

(*Continued on next page*)

| *Continued* | | |
|---|---|---|
| REAGENT or RESOURCE | SOURCE | IDENTIFIERR |
| Slc26a6 | Khamaysi et al., 2019 | RefSeq: NM_022911 |
| Software and algorithms | | |
| LECO Chroma TOF software version 4.44 | LECO Corp | N/A |
| Metalign software package | Metalign | https://www.wur.nl/nl/Onderzoek-Resultaten/Onderzoeksinstituten/food-safety-research/show-wfsr/MetAlign.htm |
| SIMCA-P+ version 12.0 | Umetrics | N/A |
| CLcommunity software | Chunlab Inc | N/A |
| Clampex 10 system | Axon Instruments | N/A |
| ImageJ | NIH | https://imagej.nih.gov/ij/ |
| FACSDiva 8.0.2 | BD biosciences | N/A |
| FlowJo 10.7.1 | BD biosciences | N/A |
| Prism 6.0 | GraphPad Inc | https://www.graphpad.com/scientific-software/prism/ |
| Other | | |
| 7890 gas chromatography system | Agilent Technologies | N/A |
| Agilent 7693 auto-sampler | Agilent Technologies | N/A |
| Pegasus® HT TOF MS | LECO Corp | N/A |
| Rtx-5MS column | Restek Corp | N/A |
| Vibra-cell Sonicator | SONICS | VCX130 |
| speed vacuum concentrator | Biotron | Modulspin 31 |
| 454 GS FLX Titanium Sequencing Systems | Roche | N/A |
| Packard 1900CA TRI-CARB | Packard | N/A |
| Amplifier | Warner Instrument Corporation | OC-725C |
| A/D converter | Axon Instruments | Digidata 1550A |
| Microscope | Olympus Optical | BX41 |
| real-time PCR | Applied Biosystems | StepOne Plus |
| FACSAria III | Becton Dickinson | N/A |
| VERSAmax tunable microplate reader | Molecular devices | N/A |
| Nanoliter 2010 injector | World Precision Instruments | N/A |

## RESOURCE AVAILABILITY

### Lead contact

Further information and requests for resources and reagents should be directed to and will be fulfilled by the lead contact, Ehud Ohana (ohanaeh@bgu.ac.il).

### Materials availability

This study did not generate new unique reagents.

### Data and code availability

- All data reported in this paper will be shared by the lead contact upon request.
- This paper does not report original code.
- Any additional information required to reanalyze the data reported in this paper is available from the lead contact upon request.

## EXPERIMENTAL MODEL AND SUBJECT DETAILS

### Human volunteers

Healthy volunteers (HC), Crohn's disease (CD) and ulcerative colitis (UC) patients of Korean heritage, were recruited at Severance Hospital (Yonsei University College of Medicine, Seoul, Korea). The Clinical and demographic characteristics of the volunteers are elaborated in Figure S3 (table 3). The Institutional Review Board of Severance Hospital, Yonsei University approved this study (IRB approval number: 4-2012-0302). All patients and controls provided written informed consent, and all methods were performed in accordance with the relevant guidelines and regulations. Patients or the public were not involved in the design, or conduct, or reporting, or dissemination of our research. Figure S3 At all times, diagnosis of CD and UC was made according to previously established international criteria based on clinical, endoscopic, histopathological, and radiological findings (Nikolaus and Schreiber, 2007).

### Animal models

All the work on mice and *Xenopus laevis* were approved by the Institutional Animal Care and Use Committee of the Ben Gurion University of the Negev, Israel (IACUC Approval No: IL-80-10-2019 and IL-83-10-2019) or Yonsei University Severance Hospital, Seoul, Korea (IACUC Approval No: 2014-0299). Colitis was induced in 8-week-old male C57BL/6 mice (Orient, Seongnam, South Korea) using DSS (2.5%, MP Biomedicals, Solon, OH, USA) or TNBS (Thermo Fisher Scientific, Pittsburgh, PA, USA), as previously described (Kim et al., 2019; Seo et al., 2017). A piece of the colons was used for metagenome analyses. All experiments using animals were carried out in accordance with the approved guidelines by the IACUC.

Peritoneal and bone marrow-derived macrophages (BMDM) were isolated from either SLC26A6$^{-/-}$ mice (Khamaysi et al., 2019; Ohana et al., 2013; Wang et al., 2006) or wild-type (WT) littermates, as described later.

### Cell cultures and transwell® system

Primary BMDM were cultured with DMEM enriched with 10% FBS, 5% L-Glutamine and pen-strep (Biological Industries, Israel), 1 mM Na-pyruvate (BMDM media). RAW264.7 cells (Schuster et al., 2020) were cultured in DMEM enriched with 10% FBS, 5% L-Glutamine and pen-strep. C2BBe1 cells (Brami et al., 2020) were cultured under similar conditions as RAW264.7 cells with the exception of adding 0.01 mg/ml human transferrin. Collagen coated transwells® (corning) were inserted in 12-well plates and incubated with DMEM. Next, Caco-2 cells and macrophages were seeded in the apical and basolateral poles, respectively. The Caco-2 culture media was replaced every 3 days during 18 to 21 days of culture.

### Bone marrow-derived and peritoneal macrophages

Hematopoietic stem cells were extracted from the femur and the tibia of 8 to 16 weeks old mice, as previously described (Amend et al., 2016). Harvested cells were cultured with 20ng/ml M-CSF (peprotech, Israel) 7 days. The remaining BMDM cells were then stimulated for 48 hours with either BMDM media alone or in the presence of 10ng/ml LPS and 20 ng/ml IFN$\gamma$ or 20 ng/ml IL4/IL13. For peritoneal cells isolation, mice were injected with thioglycolate (2% v/v, i.p., 1.5 ml per mouse). Four days later, peritoneal lavage was performed with ice cold PBS. Cells were then filtered through a 70-$\mu$m sterile nylon strainer and seeded in DMEM medium supplemented with 10% FCS, 50 units/ml penicillin, and 50 $\mu$g/ml streptomycin. Twenty-four hours later, the cells were stimulated with 10ng/ml LPS and 20 ng/ml IFN$\gamma$ for additional 24 hours.

## METHOD DETAILS

### Succinate assay of fecal samples

Succinate assay of fecal samples of healthy controls (HC), patients with Crohn's disease (CD) and with ulcerative colitis (UC), normal mice, and 2.5% dextran sulfate sodium (DSS)-treated mice with colitis was performed using succinate Colorimetric Assay Kit (MAK184, Sigma–Aldrich, MO, USA) according to the manufacturer's protocol.

### Succinate evaluation of serum samples

Metabolites were extracted from 200 $\mu$L of serum of healthy controls, patients with CD and with UC. A solution of 600 $\mu$L of methanol and 10 $\mu$L of an internal standard solution (2-chlorophenylalanine, 1 mg/mL in water) was added to the serum and then homogenized using a sonicator for 5 min. After homogenization, the suspension was held at $-20^{\circ}$C for 60 min, and then centrifuged at 12,000 rpm and 4$^{\circ}$C for 10 min. The supernatant was filtered through a 0.2-$\mu$m filter and dried using a speed vacuum concentrator (Modulspin 31; Biotron, Korea). Dried extracts were re-dissolved in 250 $\mu$L of methanol, and 100 $\mu$L of the samples were dried under a vacuum for gas chromatography (GC)–TOF–MS analysis.

For GC–TOF–MS analysis, dried samples were oximated with 50 $\mu$L of methoxyamine hydrochloride (20 mg/mL in pyridine) for 90 min at 30$^{\circ}$C and silylated with 50 $\mu$L of N-methyl-N-(trimethylsilyl) trifluoroacetamide for 30 min at 37$^{\circ}$C. GC–TOF–MS analysis was performed using an Agilent 7890 gas chromatography system (Agilent Technologies, Palo Alto, CA, USA) coupled with an Agilent 7693 auto-sampler (Agilent Technologies) and equipped with a Pegasus® HT TOF MS (LECO Corp., St. Joseph, MI, USA) system. An Rtx-5MS column (i.d., 30 m × 0.25 mm, 0.25 $\mu$m particle size; Restek Corp., Bellefonte, PA, USA) was used with a constant flow of 1.5 mL/min of helium as the carrier gas. Samples (1 $\mu$L aliquots) were injected into the GC with the splitless mode. The oven

temperature was maintained at 75°C for 2 min, then incrementally raised 15°C/min to 300°C, and finally held for 3 min. The temperatures of the front inlet and transfer lines were 250 and 240°C, respectively. The electron ionization was carried out at − 70 eV and full scanning over the range of 50–1000 m/z was used for mass data collection.

The GC–TOF–MS data were acquired and preprocessed using the LECO Chroma TOF software (version 4.44, LECO Corp.) and converted into the NetCDF format (*.cdf) using the LECO Chroma TOF software. After conversion, peak detection, retention time correction, and alignment were processed using the Metalign software package (https://www.wur.nl/nl/Onderzoek-Resultaten/Onderzoeksinstituten/food-safety-research/show-wfsr/MetAlign.htm). Multivariate statistical analysis was conducted using SIMCA-P+ (version 12.0; Umetrics, Umeå, Sweden). The dot plots of the mean of triplicate measurements were rendered using the relative peak area of unique masses of succinate by Prism 5.0 Software (GraphPad Inc. San Diego, CA, USA).

### Evaluation of microbiota changes by pyrosequencing

Total DNA from normal and inflamed colon tissues and feces of either healthy controls or IBD patients was isolated using FastDNA SPIN Kit for Soil kit (MP Biomedicals) according to the manufacturer's recommendation. Samples were collected from healthy controls, CD patients and UC patients. In addition, samples were collected from normal-water supplied mice, DSS-treated mice, and 2,4,6-trinitrobenzene sulfonic acid (TNBS)-treated mice. For pyrosequencing, amplification of genomic DNA was performed using barcoded primers that targeted the V3–V4 region of the bacterial 16S rRNA gene. The amplification, pyrosequencing, and basic analysis were performed according to the methods described by Chunlab Inc. (Seoul, Korea) (Chun et al., 2010) using a 454 GS FLX Titanium Sequencing Systems (Roche, Branford, CT, USA). Sequence reads were identified using the EzTaxon-e database (https://eztaxon-e.ezbiocloud.net/) on the basis of 16S rRNA sequence data. We analyzed operational taxonomic units (OTUs) and assessed beta diversity using principal coordinate analysis (PCoA) and alpha-diversity analysis using the diversity index (Chao1, Shannon, and Simpson index). Bacterial community abundance was generated using the CLcommunity software (Chunlab Inc.).

The OTUs for either succinate-producing or succinate-consuming bacteria were analyzed to evaluate the abundances of different species as indicated.

### Protein expression analysis by western blotting

Cell lysates were prepared by incubating the cells in an ice-cold lysis buffer containing PBS, 10 mM $Na^+$ pyrophosphate, 50 mM NaF, 1 mM $Na^+$ -orthovanadate, 1% Triton X-100, and a cocktail of protease inhibitors (Roche, Basel, Switzerland). Cells were suspended, sonicated and centrifuged. Lysates were collected and stored in SDS sample buffer. Samples were subjected to SDS-PAGE and transferred to nitrocellulose membranes (GE Whatman, Pittsburgh, PA, USA), for which western blot analysis was performed. The nitrocellulose membranes were incubated overnight with either polyclonal anti-SUCNR1, (Novusbio, Littleton, CO, USA), anti-IL-1β (Santa Cruz Biotechnology, Dallas, TX), anti-CD206 (R&D Systems, Minneapolis, USA) or anti–β-actin antibodies.

### Succinate and citrate uptake measurements

On the day of the experiment, the cells were washed with a solution that contained or lacked $Na^+$ (in mM): 5 mM KCl, 10 mM HEPES, 10 mM glucose and 140 mM NMDG-Cl ($Na^+$-free) or NaCl, pH7.4. Subsequently, the incubation solution was supplemented with radiolabeled metabolites (ViTrax Inc., Placentia, CA, USA) as follows: 1 mM succinic acid, and 1 μCi $^{14}$C-succinic acid per 1.6 μmol cold succinate or 3 mM citric acid and 1 μCi $^{3}$H-citric acid per 3 μmol cold citric acid. The 'hot' incubation solutions were added to the cells in the $Na^+$-containing (NaCl) or $Na^+$-free (NMDG-Cl) solution. The SLC13A5 inhibitor BI01383298, 1-(3,5-Dichlorophenylsulfonyl)-N-(4-fluorobenzyl)piperidine-4-carboxamide (TOCRIS Bioscience, Bristol, UK) was used at a final concentration of 10 μM. The cells were then washed twice, and NaOH (1 M) was immediately added to lyse the cells. The lysates were then transferred to scintillation vials containing HCl (1 M). Finally, radioactivity was determined by liquid scintillation counting using a Packard 1900CA TRI-CARB analyzer. The osmolarity of all solutions was adjusted to 300 mOsm with the major salt.

### Preparation and injection of oocytes

All the work on *Xenopus laevis* was approved by the Institutional Animal Care and Use Committee of the Ben Gurion University of the Negev. Oocytes were obtained by a partial ovariectomy of female *Xenopus laevis* (*Xenopus* One, Dexter, MI), as previously described (Shcheynikov et al., 2004). Briefly, the frogs were anesthetized and follicle cells were removed in an OR-2 calcium-free medium. The defolliculated oocytes were washed with OR-2 calcium-free medium and healthy oocytes in stages V to VI were identified, collected under binoculars and maintained overnight at 18°C in an ND96 solution. 32 nL of the different cRNA were injected into the oocytes using a Nanoliter 2010 injector (World Precision Instruments, Inc., Sarasota, FL). Similar volumes and concentrations (4 μg/μl) of cRNA or water were mixed to achieve similar amounts of injected cRNA per oocyte. The oocytes were incubated at 18°C in an ND96 solution with pyruvate and antibiotics and were studied 48–96 h after cRNA injection. The use of several oocyte batches may result in functional variance as we observed. To overcome this technical obstacle we monitored the currents in oocytes injected with either water or SLC13A3 in the absence or presence of slc26a6 and summarized the data for each batch.

### Voltage and current measurement in oocytes

Voltage and current recordings were performed with a two-electrode voltage clamp as described (Hong et al., 2013). The current was recorded with a Warner Instrument Corporation amplifier model OC-725C (Hamden, CT) and digitized via an A/D converter (Digidata

1550A; Axon Instruments, Inc.). The electrodes were backfilled with a 3M KCl solution. During measurements, two channels were used to record and control the membrane potential. Data were analyzed using the Clampex 10 system (Axon Instruments, Inc.). The following solutions were used as indicated in the figures: Standard HEPES-buffered ND96 oocyte regular medium containing (in mM): 96 NaCl, 2 KCl, 1.8 $CaCl_2$, 1 $MgCl_2$, and 5 HEPES, pH = 7.5. $Na^+$-succinate was added to the solutions as indicated in the figures.

### Immunohistochemistry and immunofluorescent staining

Immunohistochemistry (IHC) was performed using the following antibodies: anti-human SUCNR1 (1:200; Abbexa, Cambridge, UK), anti-human SLC26A6 (1:200, Santa Cruz Biotechnology, Santa Cruz, CA, USA). High-temperature antigen retrieval was performed by immersing the slides in a water bath at 95–98°C in a 10 mM trisodium citrate buffer (pH 6.0) for 45 min. Nonspecific binding was blocked by incubating sections for 1 h with normal horse serum (Vector, Bretton, UK) diluted in PBS. Samples were blocked for endogenous peroxidase activity using 1% $H_2O_2$ in IHC. After overnight incubation at 4°C with primary antibodies, slides were washed with PBS and incubated with anti-rabbit 1:500 or anti-mouse 1:500 secondary antibodies (Santa Cruz Biotechnology), as previously described (Seo et al., 2017). The nuclei were counterstained with 4'-6-diamidino-2-phenylindole (DAPI) in immunofluorescent staining. Images were obtained using a microscope (Olympus BX41; Olympus Optical, Tokyo, Japan). Densitometric analysis was performed using ImageJ software (NIH, Bethesda, MD, USA).

### Quantitative real-time reverse-transcription polymerase chain reaction (qRT-PCR)

Total RNA was extracted from human colon biopsies using TRIzol Reagent (Thermo Fisher Scientific, MA, USA), and 1 μg of RNA was reverse-transcribed using the High-Capacity cDNA Reverse Transcription Kit (Applied Biosystems, Foster City, CA, USA) according to the manufacturer's protocol. The cDNAs were mixed with SYBR Green master mix (Applied Biosystems) and pairs of primers (200 nmol of each primer, final concentration) in duplicate. Real-time PCR primers are as follows: Human *SLC26A6*: forward 5′-CACCTCCCGGTTTTGGTCTG-3′, reverse 5′-CAGGCCGGATAACAGGTCAC-3′; human *SLC26A3*: forward 5′-AGATGCCCCACTACTCTGTCCT-3′, reverse 5′-ATCCACACCACACCTCTGCTT-3′; human *SLC13A3*: forward 5′-CTTCATGCTCCCGGTCTCAAC-3′, reverse 5′-GCCCAGGTATTCATAGCCAAA-3′; human *SUCNR1*: forward 5′-GGAGACGTGCTCTGCATAAG-3′, reverse 5′-AGGTGTTCTCGGAAAGGATACTT-3′; human *β-ACTIN*: forward 5′-hCTCTTCCAGCCTTCCTTCCTG-3′, reverse 5′-CAGCACTGTGTTGGCGTACAG-3′. Samples were amplified in a StepOne Plus real-time PCR system (Applied Biosystems) for 45 cycles using the following PCR scheme: 95°C for 30 s, 58–61°C for 30 s, and 72°C for 40 s. Finally, gene expression levels were calculated using the relative comparative method using the following equation: relative gene expression = $2^{-(\Delta Ct\ sample - \Delta Ct\ control)}$ and results were reported as the fold change compared to the calibrator or $2^{\Delta Ct}$ after normalization of the transcript level to the average of the endogenous control, *β-ACTIN*.

### Flow Cytometry

To analyze cell surface expression of Macrophages polarization we harvested cells using Versena Solution (Life Technologies, CA, USA). Blocking was done using 1μg/ml anti-mouse CD16/CD32 (Clone 2.4G2, Biogems, CA, USA) for 10 minutes. Surfaces staining was done using 1-2μg/ml of the following antibodies; Anti-Mouse F4/80 APC (Clone BM8.1, Biogems, CA, USA), Anti-Mouse CD11b PE-Cy7 (Clone M1/70, Biolegend, CA, USA), Anti-Mouse CD80 BV421 (Clone 16-10A1, Biolegend, CA, USA) in staining buffer contains 1x PBS, 2% Fetal Bovine Serum, 0.05% Sodium Azide for 40 minutes on ice. Cells were washed with 1x PBS and analyzed using FACSAria III (Becton Dickinson, CA, USA) with appropriate detectors voltage and compensation adjustments (Software version FACSDiva 8.0.2). Samples viability (dead cells < 5%) was verified in separate sample using Propidium Iodide staining in separate tube. Data were analyzed and plotted using FlowJo (FlowJo LLC, OR, USA).

### Nitric Oxide (NO) quantification assay

NO concentrations were measured in media collected from either BMDM or RAW264.7 macrophages cultures. Briefly, the macrophage cultures were either stimulated by 10 ng/ml LPS, 20 ng/ml IFNγ, and 5 mM $Na^+$-succinate or vehicle alone (naive), and incubated for 16 hours. Subsequently, the cultures were washed with growth media containing either NaCl or $Na^+$-succinate and incubated for 50 h. During the incubation period, 65 μL of media were collected for NO analysis at different time points, as indicated in Figure 1E. The collected media samples were centrifuged for 5 min at 10,000 RPM and the supernatants were stored at −20C. A colorimetric Griess reagent system (Promega, Maddison, WI, USA) was utilized to monitor NO ($NO_2^-$) concentrations, according to the manufacturer's protocol. Colorimetric measurements were performed using the VERSAmax tunable microplate reader (Molecular devices).

## QUANTIFICATION AND STATISTICAL ANALYSIS

Prism Software (ver 5.0 and 6.0) (GraphPad Inc. San Diego, CA, USA) was used for statistical data analyses, with a two-tailed Student's t test or Mann-Whitney. For three or more groups we performed normality tests followed by the appropriate ANOVA multiple comparison tests (Tukey's, Kruskal-wallis or Dunn's). The P values, tests and statistical significance are described in the figure legends and figures. All N represent either individual samples from different patients or mice, individual wells for cell culture experiments or individual cells in the *Xenopus* oocytes experiment (Figure 2E).